Supercritical carbon dioxide extraction of *Calendula officinalis*: kinetic modeling and scaling up study

Alexis López-Padilla, Alejandro Ruiz-Rodriguez*, Guillermo Reglero and Tiziana Fornari

Institute of Food Science Research CIAL (CSIC-UAM) – CEI UAM + CSIC, Madrid, 28049, Spain;

* Correspondence: alejandro.ruiz@uam.es; Tel.: +34 -910-017-923

Abstract

The extraction of marigold (*Calendula officinalis*) oleoresin with supercritical carbon dioxide $SCCO_2$ was carried out in a small scale extraction vessel (2.7×10^{-4} m^3) studying different extraction pressures (14, 24 and 34 MPa) and different flow rates (15, 30 and 45 $g\cdot min^{-1}$) at 313 K. Then, using semi-empirical engineering scaling criteria (constant solvent lineal velocity or constant solvent residence time) and the Broken and Intact Cell (BIC) model, the scaling up to larger extraction vessels (1.35×10^{-3} m^3 and 5.16×10^{-3} m^3) was theoretically investigated.

According to the BIC model, by keeping constant the CO_2 residence time in the different size vessels a good reproduction of the kinetic behavior should be obtained. Nevertheless, experimental results did not confirm model predictions, and in fact none of the scaling criteria studied resulted adequate in the marigold supercritical extraction scaling up. Thus, using all the experimental overall extraction curves obtained, a new specific correlation was developed between the Schmidt number (Sc), CO_2 mass flow, bed geometry and the supercritical mass transfer coefficients k_{YA} with a good fit ($R^2 = 0.9767$) for scaling up the supercritical extraction of marigold.

Keywords: Supercritical fluid extraction; *Calendula officinalis*; Extracts; Scale up

1. Introduction

Marigold (*Calendula officinalis)* is an herbaceous ornamental plant native from the south of Europe. Due to its biological active compounds and its medicinal value it is cultivated all around the world on commercial scale [1,2]. *C. officinalis* flower is widely used in traditional and folk medicine and its extracts possess main biological activities such as anti-inflammatory, antitumorgenic, antiviral and cicatrizing properties [3–7]. Thus, the production of marigold extracts rich in bioactive compounds has great interest for different industries, including cosmetic, pharmacy and the food industry.

Under the concept of green processing, and considering the lipophilic character of most marigold bioactive compounds, supercritical fluid extraction (SFE) using carbon dioxide (CO_2) is one of the most efficient and promising alternatives to produce marigold extracts. SFE technology can be awarded as a superior extraction technique for biomolecules because it is organic solvent free, adequate for thermo-sensitive species, avoid oxidation damage, and can be applied from analytical scale (grams) to large industrial scale (tons) [8,9].

Regarding marigold SFE, there are many published works providing data about extraction yield, so as chemical and/or biological characterization of the extracts, obtained at different process conditions, from analytical to pilot scale. In this sense, Garcia-Risco et al. [10] studied the SFE of marigold flower on pilot scale with bed extraction volumes of 2×10^{-3} m^3 and extraction conditions of 14 MPa and 313 K, with CO_2 flow rates of 1.2×10^{-3} $kg\cdot s^{-1}$ and a total extraction time of 180 min. They reported a global extraction yield of around 3 % as well as good biological activities of the extracts, suggesting they might be used as a source of potential antiproliferative agents. Under the same experimental conditions Martin et al. [11] made the characterization of the extracts and observed a high bioaccesibility and an improved antioxidant activity after *in vitro* digestion in the terpene fraction. On the other

hand, Hamburger et al. [12] described a method for triterpenoid esters purification from *C. officinalis* flowers using a combination of SFE and chromatography. The SFE was carried out on a pilot scale with bed extraction volumes of 7.0×10^{-3} m^3, at 50 MPa, and 323 K, with CO_2 flow rates of 9.7×10^{-3} $kg \cdot s^{-1}$ and a total extraction time of 180 min. At the end of the process, a global yield of 5 % and an extract that contained 85 % faradiol of the total ester fraction were attained. One work from Baunmann et al. [13] reported the SFE of marigold from a small scale (bed extraction volumes of 9×10^{-6} m^3, with temperature and pressures of 323 K and 30, 50 and 68.9 MPa, respectively, with extraction times of 90 – 180 min).The global yields ranged from 5.5 % to 8.3 %, depending on the extraction pressure. The authors also studied the effect of scaling up to a pilot plant scale with bed extraction volumes of 7.0 $\times 10^{-3}$ m^3, concluding that a qualitative and quantitative improvement can be obtained by increasing the pressure and by adding a small amount of an extraction modifier, i.e. 0.5 % (v/v) of ethanol; nevertheless, the extraction yield decreased when the scale up was made. An analytical extraction of *C. officinalis* oleoresin (bed extraction = 1×10^{-5} m^3, P = 30, 35 and 40 MPa, T = 303, 408, 333, 348 K, extraction time = 240 min, average particle size = 190 – 220 μm) was described by Palumpitag et al. [14]. The authors recovered 87 % of lutein fatty acid esters using palm oil as modifier (10 vol.%) and obtained up to 157 mg of free lutein/g oleoresin after saponification. In the same way, Danielski et al. [4] carried out the SFE of an oleoresin from marigold flowers coming from Brazil at laboratory scale with global yields obtained in the range of 2.1 – 3.54 %, authors found that extraction yield were affected by the origin of the plant and the extraction conditions. Finally, Baratto and Riva [15] described in their patent application a process to obtain a supercritical CO_2 extract from European origin *C. officinalis* flowers and its application in cosmetic and pharmaceutical products. The inventors worked on industrial scale with 170 kg of dried marigold with 5 % of moisture content and an average particle size between 2 and 5 mm, a pressure range

between 60 and 70 MPa, and temperatures comprised between 333 and 343 K, with a total extraction time of 230 min, reporting a global extraction yield of 3 % (w/w).

Although SFE has been an important field of research within last decades, and a lot of information about extracting bioactive compounds from natural resources has been published [16,17], there is a need of more scientific studies about the influence of process variables on the extraction kinetics, the modeling of extraction curves and, particularly, the progression of scaling up strategies.

The SFE of solid materials is a semi-continuous process in which extraction time plays a central role. The mass extracted varies with time and the plot of the extraction yield vs. time is usually denoted as Overall Extraction Curve (OEC). Nevertheless, not only extraction yield, but also composition, physicochemical and biological properties of the extract vary along extraction time [18,19].

Regarding the OEC modeling, it can be pointed out that a number of kinetic models can be found at present in specialized scientific literature, including semi-empirical, simplified and comprehensive phenomenological models [16,20]. In this respect, Campos et al. [21] applied several models to represent the kinetic behavior of the extraction of marigold oleoresin with liquid and supercritical CO_2. These models include the Sovová model [22], the logistic model presented by Martínez et al. [23], the desorption model proposed by Tan and Liou [24], the simple single plate model of Gaspar et al. [25] and the diffusion model proposed by Crank and presented by Reverchon [17]. Campos et al. [21] applied all these models to represent experimental OECs, at pressures ranging from 12 to 20 MPa and temperatures from 293 to

313 K, and concluded that all models fitted reasonably well the marigold SFE experimental data.

On the other hand, more limited works are available in the literature regarding SFE scaling up studies and only a few of them described the five empirical criteria most used for scaling up processes which comprise keeping constant the following quantities: (i) ratio between the masses of spent CO_2 and biomass, (ii) ratio between CO_2 flow rate and biomass weight, (iii) a combination of both criteria (iv) a combination of both criteria plus the dimensionless Reynolds number and (v) bed geometrical relationships (height/diameter) [26]. Maintaining the same solvent linear velocity or the same solvent residence time in extraction vessels of different size, are criterions frequently investigated [27–30]. Bed geometry is considered an important factor in industrial extraction processes and the ratio between bed height (L) and bed diameter (D) has been used to validate some scale up process. For example, Carvalho et al. [31] and Zabot et al. [19, 22] applied the solvent to feed mass ratio criterion (Q/F) combined with the bed geometrical ratio (L/D), to compare the kinetic behavior in the SFE of rosemary (*Rosmarinus officinalis)* and clove buds (*Eugenia caryophyllus*), respectively, and found good results for maintaining the same (Q/F) criterion. On the other hand, Prado et al. [32] described the SFE scale up process from laboratory to pilot scale of grape seeds based on L/D ratio and found a good reproducibility of the extraction curves. Recently, Paula et al. [33] evaluated, at laboratory scale, the effect of bed geometry ratio combined with the empirical criterions of constant residence time and constant CO_2 velocity in the scaling up SFE process for *Baccharis dracunculifolia* and found that the second one was a suitable scale up criterion. And in the same year, Fernández-Ponce et al. [34] considered to keep constant

147 $\left(\frac{Q \times D}{F}\right)$ and found a suitable OEC kinetic reproduction from small scale to pilot scale
148 supercritical extraction of *Mangifera indica* leaves. In general, there is not a single criterion
149 for SFE scaling up that can be effectively applied to all systems. For example, keeping the
150 same residence time of the solvent inside the packed bed was successfully applied for the
151 SFE of *E. caryophyllus* but did not result adequate for the SFE of vetiver roots [28], showing
152 that scale up data in SFE has a big variation and sometimes there is no an easy way to find a
153 generalized conclusion between them. More studies are required to get more information
154 about the applicability of SFE scale up criteria with different types of raw materials and
155 taking account that mass transfer behavior could be affected by the origin, species and even
156 the parts of the plant involved in the SFE process [35,36]. In this respect, as cited above, a
157 few papers have been published regarding the SFE of marigold from laboratory to pilot or
158 industrial scale but none of them describe or involve a scaling up process or criteria. In this
159 work, the supercritical CO_2 extraction of marigold flowers was studied using three different
160 volumes of extraction vessels. The modeling of the extraction curves and the correlation of
161 parameters obtained were investigated in order to put forward a scaling up strategy.
162
163

164 **2. Materials and Methods**

165 **2.1 Fundamentals**

166 **2.1.1 The Broken and Intact Cells model**

167 One of the kinetic models most used to represent the OEC of SFE processes is the Broken
168 and Intact Cells (BIC) model developed by Sovová [22]. In the BIC model the solid phase is

considered to be comprised by broken and intact cells and thus the total extractable material is distributed as easily accessible solute, which is available on the surface of the broken cells, and difficultly accessible solute which is confined in the intact part of the cells. Furthermore, in the BIC model it is assumed that temperature and pressure are constant during the whole extraction time, particle size and solute distribution are uniform in the packed bed, the void fraction is constant during the extraction, and axial dispersion can be neglected (plug flow is supposed). Then, three different extraction periods are distinguished:

1. The constant extraction rate (CER) period, in which the extraction rate is constant and determined by the convective solvent film resistance.
2. The falling extraction rate (FER) period, in which the intra-particle diffusion starts to become important and thus, the extraction rate drops rapidly. At the end of this period, all the readily accessible solute has been removed from the vegetal matrix.
3. The diffusion controlled (DC) period, in which mass transfer is mainly dominated by diffusion film resistance inside the solid vegetal particles.

The BIC model equations to calculate the cumulative mass of extract (m) as a function of time (t) in the different periods are the following [22]:

CER period: $$m = QY^*\left[1-\exp(-Z)\right]t \quad (1)$$

FER period: $$m = QY^*\left[t - t_{CER}\exp(Z_w - Z)\right] \quad (2)$$

DC period: $$m = m_{SI}\left\{X_o - \frac{Y^*}{W}\ln\left[1+\left[\exp\left(\frac{WX_o}{Y^*}\right)-1\right]\exp\left[\frac{WQ(t_{CER}-t)}{m_{SI}}\right]\left(\frac{X_k}{X_o}\right)\right]\right\} \quad (3)$$

where:

$$Z = \frac{m_{SI}k_{YA}\rho}{Q\,(1-\varepsilon)\rho_s} \quad (4)$$

$$W = \frac{m_{SI} k_{XA}}{Q\,(1-\varepsilon)} \tag{5}$$

$$Z_W = \frac{ZY^*}{WX_o} \ln\left\{ \frac{X_o \exp\left[WQ\,(t - t_{CER})/m_{SI}\right] - X_k}{X_o - X_k} \right\} \tag{6}$$

$$m_{SI} = X_o F \tag{7}$$

$$t_{CER} = \frac{m_{SI}(X_o - X_k)}{Y^* ZQ} \tag{8}$$

$$t_{FER} = t_{CER} + \frac{m_{SI}}{QW} ln\left[\frac{X_k + X_p \exp(WX_o/Y^*)}{X_o}\right] \tag{9}$$

The mass ratio of the extracted material at the bed outlet (Y_{CER}) in CER period is given by:

$$Y_{CER} = \frac{m_{(t=t_{CER})}}{Qt_{CER}} \tag{10}$$

Consequently, the extraction rate at CER period is:

$$M_{CER} = Y_{CER} Q \tag{11}$$

Process parameters required to apply BIC model are the bed porosity (ε), mass (F) and density (ρ_s) of the raw material, CO_2 density (ρ) and mass flow rate (Q). Additionally, the solubility of the extract in the supercritical solvent (Y^*) and the global extraction yield (X_o) have to be determined to apply the BIC model. Parameters which are optimized according to the experimental kinetic data are the intra-particle solute ratio (X_k) and the fluid phase and solid phase volumetric mass transfer coefficients, $k_{YA} = k_f \cdot a_o$ and $k_{XA} = k_s \cdot a_o$. k_f and k_S are, respectively, the fluid and solid mass transfer coefficients and a_o is the particles surface area ($a_o = 6 \cdot (1-\varepsilon) \cdot d_p^{-1}$). The ready accessible solute (X_p) is calculated as the difference (X_o - X_k).

2.1.2 Scaling up criterions

Despite extraction temperature and pressure are crucial to establish the thermodynamic boundaries of the extraction process, affecting fundamentally the supercritical solvent density

and the solubility and diffusivity of the solutes, the CO_2 flow (i.e. the solvent velocity through the extraction cell) is a determining factor regarding mass transfer. Of course, mass transfer is also greatly influenced by bed geometry and packing, since these variables determine the mass ratio of extracted material to spent CO_2 at bed outlet.

The objective of scaling up the SFE of solid materials is to reproduce the OEC in extraction vessels of different shape and/or capacity. In general, extraction vessels are cylindrical and thus length (L) and internal diameter (D) of the cylinder are the variables which characterize bed geometry. Yet, thermodynamic process variables, temperature and pressure, are maintained the same in the different volumes vessels. Furthermore, particle size, bed density and porosity, are intended to be preserved in SFE process scaling up. Thus, the key request is to determine the CO_2 flow rate necessary to attain the same OEC in the different scale systems.

Among different approaches, two engineering rules of thumb are often applied in SFE processes to estimate the relation between the CO_2 mass flow rate (Q) and the bed geometry [29,37,38]. One of these criteria is keeping the same solvent velocity (v) in the different scale vessels 1 and 2:

$$\frac{Q_1}{Q_2} = \left(\frac{D_1}{D_2}\right)^2 \tag{12}$$

Equation (12) was obtained considering that the same temperature and pressure (same CO_2 density) are preserved in the different scale experiments 1 and 2, and that the cross-flow area of each cylindrical extraction vessel is given by $A = \pi D^2/4$.

230 The second scaling up criteria usually used is keeping the solvent residence time (t_R)
231 constant, which is calculated as the ratio between the mass of CO_2 fit in the extraction vessel
232 ($\pi D^2 L\varepsilon\rho/4$) and the CO_2 flow mass rate (Q):

233 $$t_R = \frac{\pi D^2 L\varepsilon\rho}{4Q} \quad (13)$$

234 Considering, as in previous case, that the same temperature and pressure are preserved in the
235 different scale experiments, the residence time criterion requires that:

236 $$\frac{Q_1}{Q_2} = \left(\frac{D_1}{D_2}\right)^2 \left(\frac{L_1}{L_2}\right) \quad (14)$$
237

238 **2.2 Plant material**

239 Dried marigold (*Calendula officinalis*) flowers with a moisture content of 11.8 % were
240 obtained from Murciana Herboristería (Murcia, Spain). According to supplier, the origin of
241 marigold plant was Egypt. Flowers were ground in a grind Premil 250 (Lleal S.A., Barcelona,
242 Spain) to particles sizes in the range from 175 to 1340 μm, with a mean particle size of 541
243 μm, measured by light scattering with a laser diffraction system Mastersizer 3000 (Malvern
244 Instruments Ltd., Malvern, UK), equipped with the Aero S dispersion unit at 0.5 bar of
245 dispersion pressure. The plant material density (ρ_s) was determined using a helium
246 pycnometer Ultrapyc 1200e (Quantachrome, Florida, USA) and resulted to be 1409 $kg \cdot m^{-3}$.
247 Samples were packed and stored at room temperature until utilization.

248 **2.3 Chemical**

249 Ethanol absolute (99.5 % of purity) was purchased from Panreac (Barcelona, Spain). CO_2
250 was supplied by Carburos Metalicos, S.A. (Madrid, Spain) with a purity of 99.9 %.

251 **2.4 Supercritical fluid extraction**

252 *Calendula officinalis* extractions were carried out using three cylindrical extractor vessels of
253 different capacities which were integrated in two supercritical extraction plants. Each plant

254 comprises a recirculation system where CO_2 is condensed, pumped up to the desired
255 extraction pressure and heated up to the desired extraction temperature.
256 One pilot supercritical plant (Figure 1a) is from Thar Technology (model SF2000; Pittsburgh,
257 Pensilvania, USA) with the possibility of being operated using two extraction vessels, namely
258 vessel A (V_A) of 2.7×10^{-4} m^3 (small scale experiments) and vessel B (V_B) of 1.35×10^{-3} m^3
259 (medium scale experiments). CO_2 flow is measured using a flow meter from Siemens AIS
260 (Model: Sitrans FC Mass 2100 DI 1.5, Nordborgvej, Denmark). The SFE device has a
261 computerized PLC-based instrumentation, including a separator with control of temperature
262 and pressure, where decompression up to recirculation pressure takes place. The pressure in
263 the extraction cell is controlled (± 0.1 MPa) by an automated back pressure regulator (BPR)
264 valve. Temperature is adjusted by electric heating and controlled by ± 2 K.
265 The other semi-industrial scale supercritical plant is from Zean Consultores S.L. (Madrid,
266 Spain) with an extraction vessel namely C (V_C) of 5.19×10^{-3} m^3 of capacity (large scale
267 experiments). The equipment comprises a LEWA LDE1 pump (LEWA GmbH, Leonberg,
268 Germany) with a maximum CO_2 flow rate of 146.93 $kg\cdot h^{-1}$. The pressure in the extraction
269 vessel is controlled by an automated BPR valve (RCV 2945) from Badger Meter Inc. (Tulsa,
270 USA). The cyclonic separator has a capacity of 1.57×10^{-3} m^3 with temperature and pressure
271 control from Link Industrial S.L. (Rubi, Spain). The cooling system connects the CO_2 pump
272 and the CO_2 recirculation system with two chillers Huber UC100T Advanced from Peter
273 Huber Kältemaschinenbau GmbH (Offenbur, Germany). A heating bath Huber Hotbox
274 HB120 from Peter Huber Kältemaschinenbau GmbH (Offenbur, Germany) is connected on-
275 line with the Heat Exchanger unit. The plant also comprises a demister unit with 1.5×10^{-2} m^3
276 of capacity from Proycon Pirineo S.L. (Huesca, Spain) designed to separate liquid or solid
277 particles from the outgoing stream before driving CO_2 to the storage tank and on-line
278 connected with an activated carbon filter with a capacity of 5×10^{-2} m^3. The semi-industrial

279 supercritical device has a PLC-based instrumentation and control from Invensys S.L.
280 (Madrid, Spain). A scheme of Zean supercritical plant is given in Figure 1b.

281 **2.4.1 Small scale experiments**

282 Kinetic behavior was studied in a small scale vessel (V_A), packed with 0.090 kg of grinded
283 marigold flowers. OECs were obtained at 313 K and pressures of 14, 24 and 34 MPa, with a
284 CO_2 flow of 5.0×10^{-4} kg·s^{-1}. Furthermore, additional OECs were obtained at constant
285 pressure (14 MPa) and temperature (313 K) and CO_2 flows of 2.5×10^{-4}, 5.0×10^{-4} and 7.5×10^{-4}
286 kg·s^{-1}, respectively. Extraction conditions of all OECs which were carried out in V_A are
287 summarized in Table 1.
288 The first sample was collected after 15 min of extraction, second data point at 30 min, and
289 the rest of the data were collected at intervals of 60 min until 180 min and the last one was
290 collected at 270 min of total extraction time. Additionally, at 14 MPa, 313 K and 5.0×10^{-4}
291 kg·s^{-1} CO_2 samples were collected in the separator until the vegetal material was completely
292 extracted (750 min).
293 In all experimental assays the supercritical stream was decompressed at 5.4 MPa (i.e. the
294 recirculation system pressure) in the separator. The different samples were collected with
295 ethanol which was eliminated at low temperature (313 K) in a rotavapor R210 (Büchi
296 Labortechnik AG, Flawil, Switzerland).

297 **2.4.2 Medium scale experiments**

298 V_B was used with 0.445 kg of ground marigold flowers, see Table 2. Extraction pressure and
299 temperature were 14 MPa and 313 K, and the CO_2 flow rate was set to 6.0×10^{-4} kg·s^{-1} or
300 12.3×10^{-4} kg·s^{-1} according to the results of the scaling criterion adopted (Eq. 12 or Eq. 14,

301 respectively). Samples at 15, 30, 60, 120, 180 and 270 min of extraction were collected in
302 the separator with ethanol, and the solvent was eliminated at 313 K in the rotavapor.

303 **2.4.3 Large scale experiments**

304 Large scale experiments were carried out in extraction vessel V_C with 1.708 kg of marigold
305 flowers as can be observed in Table 2. The extraction pressure and temperature were identical
306 to those used for scaling studies (14 MPa and 313 K) in vessels A and B. The CO_2 flow rate
307 was set to 21.2×10^{-4} kg·s^{-1} according to the constant linear velocity criterion (Eq. 12) or to
308 46.8×10^{-4} kg·s^{-1} considering the constant residence time scaling criterion (Eq. 14). The
309 extracts were collected from the separators at 60, 120, 180 and 270 min of total extraction
310 using ethanol which was evaporated after in a rotavapor.

311

312 **3. Results and Discussions**

313 **3.1 Apparent density and porosity of the packed beds**

314 Table 2 shows the geometrical characteristics of the different extraction vessels, together
315 with the mass of marigold used in each one. The mass of grinded marigold flowers (solid
316 density ρ_s = 1409 kg·m^{-3}) loaded in each extraction vessel was calculated in order to preserve
317 the same apparent density (ρ_{app} = 333 kg·m^{-3}) and porosity (ε = 0.763) in the three packed
318 beds. The vessel loading was carried out using the same protocol, and the calculated amount
319 of vegetal material satisfactory filled the corresponding extraction vessel.

320 **3.2 Small scale OECs**

321 The overall yields are reported in Table 1 and correspond to 313 K and 270 min of extraction
322 time. The shape of the OECs obtained at different pressures and solvent flow rates are shown
323 in Figure 2. Extraction yield was calculated as the ratio between the mass extracted (m) and
324 the mass of grinded calendula flowers feed into the extraction vessel (F).

As expected, extraction yield increases with increasing pressure at constant temperature (T = 313 K) and constant CO_2 flow rate ($Q = 5.0\times10^{-4}$ kg·s^{-1}). This behavior is due the increase of the supercritical solvent density, which enlarges the solubility of the solutes and thus enhances the extraction rate. However, slight increase of global yield was observed when pressure raised from 24 to 34 MPa (from 6.11 % to 6.28 %). Additionally, the effect of CO_2 flow rate on the global yield was important when Q increased from 2.5×10^{-4} to 7.5×10^{-4} kg·s^{-1} at 14 MPa (extraction yields were 4.56 and 6.11 %, respectively).

In general, the extractions yields of *Calendula officinalis* attained in this work were considerably higher than those obtained by Campos et al. [11], which were lower than 2.5 % for marigold flowers from Brazil at 313 K and pressures in the range 12-20 MPa and large extraction times (higher than 270 min). One reason could be the different origin of marigold plant, but also the lower Q/F ratios used by Campos et al. ($0.46\text{-}0.70\times10^{-3}$ s^{-1}) in comparison with those used in this work ($2.78\text{-}8.33\times10^{-3}$ s^{-1}).

3.3 Solubility determination

Solubility data is essential information for understanding the supercritical extraction process. Accordingly, the solubility of the solute in supercritical CO_2 (Y^*) is usually a parameter in SFE kinetic models, as is the case for the BIC model.

The thermodynamic concept of solubility refers to the amount of a pure compound which can be dissolved in supercritical CO_2 at a given temperature and pressure. There are many methods proposed [39] for the experimental determination of the solute solubility (static, dynamic and chromatographic methods) and also theoretical approaches have been proposed for solubility prediction, minimizing experimental efforts and costs [40]. When the solute is a multicomponent mixture such in the case of vegetal extracts, the concept of apparent solubility is utilized which is usually determined considering the kinetic data of the initial period of the OEC. In this period, the accessibility of the extractable material results in a constant extraction rate period and hence, the slope of the linear behavior (extracted mass vs.

mass of CO_2) is used to calculate the apparent solubility of the vegetal oleoresin at the temperature and pressure extraction conditions [29,42–45].

In this work the solubility of marigold extracts in supercritical CO_2 was determined at 313 K and 14 MPa using the first stages of the OECs obtained with the different solvent flow rates. Figure 3 shows these data plotted as mass of marigold oleoresin extracted vs. mass of spent CO_2. As can be observed in the figure, the data fit a good linear behavior ($R^2 = 0.9086$) for a CO_2 mass load lower than 0.8 kg. This means that in the first stage of the OECs obtained for the supercritical solvent was saturated with the marigold extractable material and thus, the slope of this linear trend is given in Figure 3 can be considered a reasonably estimation of marigold solubility. Then, Y^* was calculated to be 0.0032 kg of marigold extract per kg of CO_2 at 313 K and 14 MPa. This value is reasonably in accordance with the value reported by Danielski [46] at 313 K and 20 MPa (0.0028 kg/kg) which was used by Campos et al. due to the lack of solubility data [11].

3.4 Total extractable material

In order to apply BIC model, the total amount of extractable material (X_o) at a given extraction temperature and pressure, has to be determined. Then, a kinetic experiment was carried out at 313 K and 14 MPa extending extraction time until the vegetal material loaded in the extraction vessel was exhausted. Figure 2 shows the OEC obtained in vessel A with a CO_2 flow rate of 5.0×10^{-4} kg·s^{-1}. After 750 min of extraction, the amount of material recovered in the separator was lower than 0.1 % of the total material extracted. In view of that, the value of X_o was estimated to be 0.1 % higher than the total yield obtained after 750 min of extraction (X_o = 0.0745 kg/kg).

3.5 BIC model fitting of small scale OECs

BIC model was used to represent the experimental data obtained in the small scale V_A extraction vessel (see Table 1 and Figure 2). Table 3 shows the optimal mass transfer coefficients (k_{YA} and k_{XA}) for each of the five OECs. The intra-particle solute ratio (X_k) was

optimized as a unique value for all the OECs. The resulted value (see Table 3) indicates that only around 40 % of the extractable material is easily accessible. Also is included in Table 3 the average absolute relative deviation (*AARD*) of each OEC fitting (< 6.62 %). Figure 2 shows with dashed lines the BIC model fitting achieved.

For the sake of comparison, the values of the mass transfer coefficients obtained are compared with those reported by Campos et al. [21] for the BIC modeling of marigold OEC at 313 K and 15 MPa, which were $k_{YA} = 0.08\times10^{-2}$ s^{-1} and $k_{XA} = 0.001\times10^{-3}$ s^{-1}. The lower values obtained in the work of Campos et al. (2005) are in accordance with the lower yields obtained and can be explained by both the lower apparent solubility and *Q/F* ratios used.

At constant temperature (313 K) and CO_2 flow rate (5.0×10^{-4} $kg\cdot s^{-1}$) the k_{YA} and k_{XA} values increase with increasing pressure and accordingly, higher extraction rates (M_{CER}) are obtained. At the three pressures investigated, the mass ratio of the extracted material at the bed outlet (Y_{CER}) is rather close to marigold oleoresin apparent solubility (i.e. the solvent is saturated with marigold extractable material), which was calculated as indicated in section 3.3 at 14 MPa ($Y^* = 0.0032$ $kg\cdot kg^{-1}$). At pressures of 24 MPa and 34 MPa, the Y^* values were considered fitting parameters and the optimal values (see Table 3) resulted very close to the slope of the corresponding OEC from t = 0 to t = 15 min, which were 0.0039 and 0.0050 $kg\cdot kg^{-1}$, respectively.

Regarding the effect of solvent flow rate, as expected, the k_{YA} values increase with increasing Q at constant pressure and temperature, and lower t_{CER} values are obtained. While Y_{CER} is very close to the extract apparent solubility, as mentioned before, increased solvent flow rates resulted in higher extraction rates (M_{CER}) and thus, the time in which ends the falling extraction rate period (t_{FER}) is shorter.

3.6 SFE scaling up study

3.6.1 BIC model prediction for marigold SFE scaling up

The BIC model was used to assess whether the solvent constant velocity (Eq. 12) or the solvent constant residence time (Eq. 14) were suitable criterions to calculate the CO_2 flow rate (Q) required for scaling up from vessel A to vessels B and C (scaling factors V_B/V_A = 4.95 and V_C/V_A = 19.04, respectively). The extraction conditions of the OEC target to be reproduced were 313 K, 14 MPa and 2.5×10^{-4} kg·s^{-1} (V_A). Bed porosity was kept constant (ε = 0.763) for all BIC simulations. The Q values calculated from Eq. (12) and (14) are given in Table 4 for each scaling case (V_B and V_C).

As can be observed in Table 4, t_{CER} is the same for all predictions regardless of the criterion applied to calculate Q. Nevertheless, the ratios $(M_{CER})_B/(M_{CER})_A$ and $(M_{CER})_C/(M_{CER})_A$ are equal to the corresponding scaling factors only when Eq. (14) was used to calculate Q. That is, according to the BIC model, the criterion given by Eq. (14) is suitable for marigold SFE scaling up from small scale (V_A) to both larger scales (V_B and V_C). Furthermore, it can be observed in Table 4 that the t_{FER} values obtained in the OEC simulations are similar only in the case of preserving the same residence time in the different scale units. That is, using Eq. (14) to Q scaling up and according to BIC simulation, the easy accessible material is completely extracted in around 73 min regardless the vessel scale.

The results of BIC simulation of the OECs at 313 K and 14 MPa in vessel B and vessel C with the different calculated Q values are depicted in Figures 5 (V_B/V_A = 4.95) and 6 (V_C/V_A = 19.04), respectively. Grey lines in the figures correspond to BIC simulation when Q is calculated according to Eq. (12), while black lines correspond to the use of Eq. (14). As can be observed for both vessel scales, black lines are the ones that fit reasonably well the experimental small scale OEC. Furthermore, in both cases, BIC model predicts that the CO_2 flow rate calculated according Eq. (12) (constant solvent lineal velocity) provides a significant delayed extraction.

3.6.2 Experimental marigold SFE scaling up

The SFE of marigold was experimentally carried out in vessels V_B and V_C with the CO_2 flow rates calculated according Eq. (12) or Eq. (14) and given in Table 4. The OECs obtained in each case are represented in Figure 4 (V_B) and Figure 5 (V_C), respectively. Despite BIC model predicts that Eq. (14) should be adequate for Q scaling up in both larger scale vessels, experimental data show important discrepancies.

In the case of V_B, similar OEC was obtained at the initial stages of the extraction when the solvent flow rate was the one provided by Eq. (14), but experimental results deviates from BIC model (and from the small scale experimental OEC) for increasing extraction time. Furthermore, the solvent flow rate obtained with Eq. (12) resulted in an OEC with significant lower yields, in comparison with BIC predictions and with the small scale experimental OEC. On the other hand, the opposite tendency is observed when scaling from V_A to V_C. The solvent flow rate calculated using Eq. (14) resulted in significant larger yields than those obtained in V_A, while the OEC obtained using Eq. (12) is quite similar to the small scale experimental OEC.

3.6.3 Correlation of experimental data for scaling up

The theoretical fundamentals of the mass transfer correlations, which relate Sherwood (Sh) with Reynolds (Re) and Schmidt (Sc) dimensionless numbers [47], were used in order to assess a relation between the fluid phase mass transfer coefficients (k_{YA}) and the solvent flow rate (Q) of all experimental OECs obtained in this work for marigold SFE. The Sc number was included to take into account the most important physicochemical parameters of the extraction which depend on temperature and pressure:

$$Sc = \frac{\mu_{CO2}}{\rho_{CO2}\ D_{M-CO2}} \quad (15)$$

ρ_{CO2} and μ_{CO2} are, respectively, the solvent density and viscosity, and D_{M-CO2} is the diffusion coefficient of marigold oleoresin in supercritical CO_2 which was calculated following the general correlation recently proposed by López-Padilla et al. [48].

Figure 6 show the correlation obtained (R^2 = 0.9767) which also include vessel geometrical dimensions (D and L). As can be observed in the figure, it satisfactory takes into account the variation of some process variables, such as pressure and solvent flow rate, at constant extraction temperature. Nevertheless, it has to be pointed out that other important variables, such as particle diameter (d_p) and bed porosity (ε), were kept constant in all OECs used in the development of this correlation. The effect of d_p and ε, and the potential extension of this type of correlation to other vegetal raw materials is in progress, in order to set a practical methodology for solid vegetal raw materials scaling up in the context of the different scale SFE units available in our pilot plant.

4. Conclusions

SFE curves of *C. officinalis* at different extraction pressure, temperature and CO_2 mass flow were measured at small scale, and were adequately represented by the BIC model. The model was then used to assess the accuracy of scaling up criteria. According to BIC model the constant CO_2 residence time criterion should provide good estimation of the CO_2 mass flow for both scaling factors of 4.9 and 19. Nevertheless, experimental results do not agree with the theoretical prediction: while the constant CO_2 residence time criterion looks quite satisfactorily for a scaling factor of 4.9, the constant CO_2 velocity was the criterion suitable for a larger scaling factor of 19.

The mass transfer coefficients in the supercritical fluid phase (k_{YA}) of all extraction curves obtained in the different size cells and applying different extraction pressure, temperature and CO_2 mass flow rate were satisfactorily correlated (R^2 = 0.9767) in terms of the CO_2 flow rate (Q), the extraction cell geometric parameters (diameter D and length L) and the dimensionless Schmidt number (Sc). This correlation should be tested in terms of parameters which were kept constant in this work, such as porosity and/or particle size.

Acknowledgments

López-Padilla A thanks to Administrative Department of Science, Technology and Innovation - Colciencias (Call 568/2012) for his Ph.D. fellowship. This work was financed thanks to ALIBIRD project: S2013/ABI-2728 (Comunidad de Madrid).

References

[1] D. Arora, A. Rani, A. Sharma, A review on phytochemistry and ethnopharmacological aspects of genus Calendula., Pharmacogn rev. 7 (2013) 179–187. http://dx.doi.org/10.4103/0973-7847.120520.

[2] R. Sausserde, K. Kampuss, Composition of Carotenoids in Calendula (*Calendula officinalis* L.) flowers, in: Foodbalt 2014, Jelgava, Latvia, 2014: pp. 13–18. http://agris.fao.org/agris-search/search.do?recordID=LV2014000480.

[3] M. Miguel, L. Barros, C. Pereira, R.C. Calhelha, P.A. García, M.A. Castro, et al., Chemical characterization and bioactive properties of two aromatic plants : *Calendula officinalis* (flowers) and *Mentha cervina* (leaves), Food Funct. 7 (2016) 2223–2232. http://pubs.rsc.org/en/content/articlepdf/2016/fo/c6fo00398b..

[4] L. Danielski, L.M.A.S. Campos, L.F. V Bresciani, H. Hense, R.A. Yunes, S.R.S. Ferreira, Marigold (*Calendula officinalis* L.) oleoresin: Solubility in SC-CO2 and composition profile, Chem. Eng. Process: Process Intensification. 46 (2007) 99–106. http://dx.doi.org/10.1016/j.cep.2006.05.004.

[5] Z. Kalvatchev, R. Walder, D. Garzaro, Anti-HIV activity of extracts from *Calendula officinalis* flowers, Biomed. Pharmacother. 51 (1997) 176–180. http://dx.doi.org/10.1016/S0753-3322(97)85587-4.

[6] A. Ramos, A. Edreira, A. Vizoso, J. Betancourt, M. López, M. Décalo, Genotoxicity of an extract of *Calendula officinalis* L., J. Ethnopharmacology. 61 (1998) 49–55. http://dx.doi.org/10.1016/S0378-8741(98)00017-8.

[7] M. Wang, R. Tsao, S. Zhang, Z. Dong, R. Yang, J. Gong, et al., Antioxidant activity,

509 mutagenicity/anti-mutagenicity, and clastogenicity/anti-clastogenicity of lutein from
510 marigold flowers, Food Chem. Toxicol. 44 (2006) 1522–1529.
511 http://dx.doi.org/10.1016/j.fct.2006.04.005.
512 [8] M.A. McHugh, V.J. Krukonis, Supercritical Fluid Extraction: Principles and Practice,
513 Butterworths, Boston, 1994.
514 [9] M. Mukhopadhyay, Natural Extracts Using Supercritical Carbon Dioxide, CRC Press,
515 New York, 2000.
516 [10] M.R. García-Risco, L. Mouhid, L. Salas-pérez, A. López-padilla, S. Santoyo, L.
517 Jaime, et al., Biological Activities of Asteraceae (*Achillea millefolium* and *Calendula*
518 *officinalis*) and Lamiaceae (*Melissa officinalis* and *Origanum majorana*) Plant
519 Extracts, Plant Foods Hum. Nutr. (2017) 1–7.
520 http://dx.doi.org/10.1016/j.supflu.2010.09.030.
521 [11] D. Martin, J. Navarro del Hierro, D. Villanueva Bermejo, R. Fernández-Ruiz, T.
522 Fornari, G. Reglero, Bioaccessibility and Antioxidant Activity of *Calendula officinalis*
523 Supercritical Extract as Affected by in Vitro Codigestion with Olive Oil, J. Agr. Food
524 Chem. 64 (2016) 8828–8837. http://pubs.acs.org/doi/abs/10.1021/acs.jafc.6b04313.
525 [12] M. Hamburger, S. Adler, D. Baumann, A. Förg, B. Weinreich, Preparative purification
526 of the major anti-inflammatory triterpenoid esters from Marigold (*Calendula*
527 *officinalis*), Fitoterapia. 74 (2003) 328–338. http://dx.doi.org/10.1016/S0367-
528 326X(03)00051-0.
529 [13] D. Baumann, S. Adler, S. Grüner, F. Otto, B. Weinreich, M. Hamburger, Supercritical
530 carbon dioxide extraction of marigold at high pressures: Comparison of analytical and

pilot-scale extraction, Phytochem. Analysis. 15 (2004) 226–230. http://dx.doi.org/doi/10.1002/pca.772.

[14] W. Palumpitag, P. Prasitchoke, M. Goto, A. Shotipruk, Supercritical Carbon Dioxide Extraction of Marigold Lutein Fatty Acid Esters: Effects of Cosolvents and Saponification Conditions, Sepa. Sci. Technol. 46 (2011) 605–610. http://dx.doi.org/10.1080/01496395.2010.533739.

[15] G. Baratto, E. Riva, Process for preparing an inflorescence extract of *Calendula officinalis* by means of extraction with supercritical carbon dioxide and compositions containing said extract, EP2520306A1, 2012.

[16] M.M.R. de Melo, A.J.D. Silvestre, C.M. Silva, Supercritical fluid extraction of vegetable matrices: Applications, trends and future perspectives of a convincing green technology, J. Supercrit. Fluid. 92 (2014) 115–176. http://dx.doi.org/10.1016/j.supflu.2014.04.007.

[17] E. Reverchon, I. De Marco, Supercritical fluid extraction and fractionation of natural matter, J. Supercrit. Fluid. 38 (2006) 146–166. http://dx.doi.org/10.1016/j.supflu.2006.03.020.

[18] G.L. Zabot, M.N. Moraes, M.A.A. Meireles, Influence of the bed geometry on the kinetics of rosemary compounds extraction with supercritical CO2, J. Supercrit. Fluid. 94 (2014) 234–244. http://dx.doi.org/10.1016/j.supflu.2014.07.020.

[19] M.R. García-Risco, E.J. Hernández, G. Vicente, T. Fornari, F.J. Señoráns, G. Reglero, Kinetic study of pilot-scale supercritical CO2 extraction of rosemary (*Rosmarinus officinalis*) leaves, J. Supercrit. Fluid. 55 (2011) 971–976.

http://dx.doi.org/10.1016/j.supflu.2010.09.030.

[20] Z. Huang, X.-H. Shi, W.-J. Jiang, Theoretical models for supercritical fluid extraction., J. Chromatogr. A. 1250 (2012) 2–26. http://dx.doi.org/10.1016/j.chroma.2012.04.032.

[21] L.M.A.S. Campos, E.M.Z. Michielin, L. Danielski, S.R.S. Ferreira, Experimental data and modeling the supercritical fluid extraction of marigold (*Calendula officinalis*) oleoresin, J. Supercrit. Fluids¡. 34 (2005) 163–170. http://dx.doi.org/10.1016/j.supflu.2004.11.010.

[22] H. Sovová, Rate of the vegetable oil extraction with supercritical CO2—I. Modelling of extraction curves, Chem. Eng. Sci. 49 (1994) 409–414. http://dx.doi.org/10.1016/0009-2509(94)87012-8.

[23] J. Martinez, A.R. Monteiro, P.T.V. Rosa, M.O.M. Marques, M.A. Meireles, Multicomponent model to describe extraction of ginger oleoresin with supercritical carbon dioxide, Ind. Eng. Chem. Res. 42 (2003) 1057–1063. http://pubs.acs.org/doi/abs/10.1021/ie020694f.

[24] C.-S. Tan, D.-C. Liou, Modeling of desorption at supercritical conditions, AIChE J. 35 (1989) 1029–1031. http://onlinelibrary.wiley.com/doi/10.1002/aic.690350616/epdf.

[25] F. Gaspar, T. Lu, R. Santos, B. Al-Duri, Modelling the extraction of essential oils with compressed carbon dioxide, J. Supercrit. Fluid. 25 (2003) 247–260. http://dx.doi.org/10.1016/S0896-8446(02)00149-3.

[26] M.M.R. De Melo, R.M.A. Domingues, M. Sova, E. Lack, H. Seidlitz, F. Lang, et al., Scale-up studies of the supercritical fluid extraction of triterpenic acids from

575 *Eucalyptus globulus* bark, J. Supercrit Fluid. 95 (2014) 44–50.
576 http://dx.doi.org/10.1016/j.supflu.2014.07.030.
577 [27] G.L. Zabot, M.N. Moraes, A.J. Petenate, M.A. Meireles, Influence of the bed
578 geometry on the kinetics of the extraction of clove bud oil with supercritical CO_2, J.
579 Supercrit. Fluid. 93 (2014) 56–66. http://dx.doi.org/10.1016/j.supflu.2013.10.001.
580 [28] J. Martínez, P.T.V. Rosa, M.A.A. Meireles, Extraction of Clove and Vetiver Oils with
581 Supercritical Carbon Dioxide: Modeling and Simulation, Open Chem. Eng. J. 1 (2007)
582 1–7. https://benthamopen.com/ABSTRACT/TOCENGJ-1-1.
583 [29] A. López-Padilla, A. Ruiz-Rodriguez, C. Restrepo Flórez, D. Rivero Barrios, G.
584 Reglero, T. Fornari, *Vaccinium meridionale* Swartz Supercritical CO_2 Extraction:
585 Effect of Process Conditions and Scaling Up, Materials. 9 (2016) 519.
586 http://www.mdpi.com/1996-1944/9/7/519.
587 [30] T. Hatami, M.A.A. Meireles, G. Zahedi, Mathematical modeling and genetic
588 algorithm optimization of clove oil extraction with supercritical carbon dioxide, J.
589 Supercrit. Fluid. 51 (2010) 331–338. http://dx.doi.org/10.1016/j.supflu.2009.10.001.
590 [31] R.N. Carvalho, L.S. Moura, P.T. V Rosa, M.A.A. Meireles, Supercritical fluid
591 extraction from rosemary (*Rosmarinus officinalis*): Kinetic data, extract's global yield,
592 composition, and antioxidant activity, J. Supercrit. Fluid. 35 (2005) 197–204.
593 http://dx.doi.org/10.1016/j.supflu.2005.01.009.
594 [32] J.M. Prado, I. Dalmolin, N.D.D. Carareto, R.C. Basso, A.J. a. Meirelles, J. Vladimir
595 Oliveira, et al., Supercritical fluid extraction of grape seed: Process scale-up, extract
596 chemical composition and economic evaluation, J. Food Eng. 109 (2012) 249–257.

http://dx.doi.org/10.1016/j.jfoodeng.2011.10.007.

[33] J.T. Paula, A.C. Aguiar, I.M.O. Sousa, P.M. Magalhães, M.A. Foglio, F.A. Cabral, Scale-up study of supercritical fluid extraction process for *Baccharis dracunculifolia*, J. Supercrit. Fluid. 107 (2016) 219–225. http://dx.doi.org/10.1016/j.supflu.2015.09.013.

[34] M.T. Fernández-Ponce, B.R. Parjikolaei, H.N. Lari, L. Casas, C. Mantell, E.J. Martínez de la Ossa, Pilot-plant scale extraction of phenolic compounds from mango leaves using different green techniques: Kinetic and scale up study, Chem. Eng. J. 299 (2016) 420–430. http://dx.doi.org/10.1016/j.cej.2016.04.046.

[35] J.M. Prado, G.H.C. Prado, M.A.A. Meireles, Scale-up study of supercritical fluid extraction process for clove and sugarcane residue, J. Supercrit. Fluid. 56 (2011) 231–237. http://dx.doi.org/10.1016/j.supflu.2010.10.036.

[36] E. Reverchon, C. Marrone, Supercritical extraction of clove bud essential oil: Isolation and mathematical modeling, Chem. Eng. Sci. 52 (1997) 3421–3428. http://dx.doi.org/10.1016/S0009-2509(97)00172-3.

[37] M.T. Fernández-Ponce, L. Casas, C. Mantell, E.J.M. De La Ossa, Potential Use of mango leaves extracts obtained by high pressure technologies in cosmetic, pharmaceutics and food industries, Chem. Eng. Trans. 32 (2013) 1147–1152. http://www.aidic.it/cet/13/32/192.pdf.

[38] L. Casas, C. Mantell, M. Rodríguez, A. Torres, F.A. Macías, E.J.M. de la Ossa, SFE kinetics of bioactive compounds from *Helianthus annuus* L, J. Sep. Sci. 32 (2009) http://onlinelibrary.wiley.com/doi/10.1002/jssc.200800663/epdf.

[39] R. Dohrn, J.M.S. Fonseca, S. Peper, Experimental methods for phase equilibria at high pressures., Ann Rev Chem Biomol. 3 (2012) 343–67. https://doi.org/10.1146/annurev-chembioeng-062011-081008.

[40] D.E. Knox, Solubilities in supercritical fluids, Pure Appl. Chem. 77 (2005) 513–530. https://doi.org/10.1351/pac200577030513.

[41] U. Salgın, S. Salgın, Effect of main process parameters on extraction of pine kernel lipid using supercritical green solvents: Solubility models and lipid profiles, J. Supercrit. Fluid. 73 (2013) 18–27. http://dx.doi.org/10.1016/j.supflu.2012.11.002.

[42] K.S. Duba, L. Fiori, Supercritical CO_2 extraction of grape seed oil: Effect of process parameters on the extraction kinetics, J. Supercrit Fluid. 98 (2015) 33–43. http://dx.doi.org/10.1016/j.supflu.2014.12.021.

[43] S.G. Özkal, U. Salgin, M.E. Yener, Supercritical carbon dioxide extraction of hazelnut oil, J. Food Eng. 69 (2005) 217–223. http://dx.doi.org/10.1016/j.jfoodeng.2004.07.020.

[44] U. Salgin, Extraction of jojoba seed oil using supercritical CO_2+ethanol mixture in green and high-tech separation process, J. Supercrit. Fluid. 39 (2007) 330–337. http://dx.doi.org/10.1016/j.supflu.2006.03.013.

[45] U. Salgin, H. Korkmaz, A green separation process for recovery of healthy oil from pumpkin seed, J. Supercrit Fluid. 58 (2011) 239–248. http://dx.doi.org/10.1016/j.supflu.2011.06.002.

[46] L. Danielski, Solubilidade das Oleoresinas de Calendula (*Calendula officinalis* L.) e Cavalinha (*Equisetum arvense*) em CO2 Supercrítico, Universidade Federal de Santa

641 Catarina, 2002.
642 [47] R.B. Bird, W.E. Stewart, E.N. Lightfoot, Transport Phenomena, in: 2nd ed., John
643 Wiley & Sons, Inc., New York, NY, 2002: p. 914.
644 [48] A. López-Padilla, A. Ruiz-Rodriguez, G. Reglero, T. Fornari, Study of the diffusion
645 coefficient of solute-type extracts in supercritical carbon dioxide: Volatile oils, fatty
646 acids and fixed oils, J. Supercrit. Fluid. 109 (2016) 148–156.
647 http://dx.doi.org/10.1016/j.supflu.2015.11.017.
648 [49] NIST, Thermophysical properties of fluid systems, National Institute of Standards and
649 Technology. (2016). http://webbook.nist.gov/chemistry/fluid/ (accessed December
650 18, 2016).
651
652

Table 1. Total extraction yield (extraction time = 270 min) obtained in the SFE of *Calendula officinalis* at 313 K and different pressures and CO_2 mass flow rates and extraction vessels with a bed porosity of $\varepsilon = 0.763$.

Run order	Scale	$Q \times 10^4$ (kg·s^{-1})	P (MPa)	Yield (%)
1	V_{A1}	2.5	14	4.56
2	V_{A2}	5.0	14	5.61
3	V_{A3}	7.5	14	6.11
4	V_{A4}	5.0	24	6.28
5	V_{A5}	5.0	34	6.48
6	V_{B1}	6.0	14	3.08
7	V_{B2}	12.3	14	4.15
8	V_{C1}	15.5	14	4.77
9	V_{C2}	47.0	14	7.38

Extraction vessels volume: V_{A1} to $V_{A5} = 2.7\times10^{-4}$ m^3; V_{B1} and $V_{B2} = 1.35\times10^{-3}$ m^3; V_{C1} and $V_{C2} = 5.19\times10^{-3}$ m^3.

659 **Table 2.** Geometrical characteristics of the cylindrical extraction vessels used in this work
660 and mass of grinded marigold flowers loaded in each extraction vessel.
661

	V_A	V_B	V_C
Internal diameter, D (m)	0.043	0.067	0.107
Length, L (m)	0.188	0.383	0.570
L/D ratio	4.372	5.716	5.327
Cross-flow area, A (m^2)	0.00145	0.00353	0.00899
Volume, V (m^3)	0.00027	0.00135	0.00519
Mass loaded, F (kg)	0.090	0.445	1.708

662

663 **Table 3.** Optimal parameters obtained in the OEC fitting (BIC model) of the small scale
664 (vessel V_A) marigold SFE at 313 K and different CO_2 flow rates and extraction pressures. V_A
665 = 2.7×10^{-4} m^3; F = 0.090 kg; ε = 0.763; X_o = 0.0745; X_k = 0.0450.
666

	P = 14 MPa			P = 24 MPa	P = 34 MPa
Run order	1	2	3	4	5
$Q \times10^4$ ($kg\cdot s^{-1}$)	2.5	5.0	7.5	5.0	5.0
ρ_{CO2}* ($kg\cdot m^3$)	763.2	763.2	763.2	872.5	930.2
Y* ($kg\cdot kg^{-1}$)	0.0032	0.0032	0.0032	0.0038**	0.0049**
$k_{YA} \times 10^2$ (s^{-1})	0.420	0.570	0.940	0.97	1.50
$k_{XA} \times 10^3$ (s^{-1})	0.010	0.021	0.027	0.039	0.055
t_{CER} (mim)	15.98	11.78	7.14	5.10	2.40
t_{FER} (mim)	72.34	40.08	25.75	30.3	22.17
Y_{CER} (kg/kg)	0.0031	0.0028	0.0029	0.0036	0.0048
$M_{CER} \times 10^7$ ($kg\cdot s^{-1}$)	7.68	14.2	21.8	18.3	24.3
*AARD**** *(%)*	6.62	3.67	2.06	2.47	5.06

667 * [49]
668 ** fitting parameter
669 ***$AARD = \frac{1}{N}\sum\left|\frac{calculated\ yield - experimental\ yield}{experimental\ yield}\right|$
670
671
672

673 **Table 4.** Marigold SFE scaling up (BIC model predictions) at 14 MPa and 313 K from the
674 small extraction vessel (V_A) to two larger scale vessels (V_B and V_C) preserving bed porosity
675 ($\varepsilon = 0.763$). CO_2 flow rates were calculated according to Eq. (12) (equal CO_2 linear velocity)
676 or Eq. (14) (equal CO_2 residence time) scaling criteria.
677

	V_A	V_B		V_C	
		Eq. (12)	Eq. (14)	Eq. (12)	Eq. (14)
Run order	1	6	7	8	9
L/D	4.372	5.716	5.716	5.327	5.327
Q $\times 10^4$ ($kg \cdot s^{-1}$)	2.5	6.0	12.3	15.5	47.0
$v \times 10^4$ ($m \cdot s^{-1}$)	2.25	2.25	4.58	2.25	6.85
t_R (min)	10.6	21.8	10.6	32.1	10.6
t_{CER} (min)	15.98	15.98	15.98	15.98	15.98
t_{FER} (min)	72.3	145.3	73.1	221.6	72.9
$M_{CER} \times 10^7$ ($kg \cdot s^{-1}$)	7.68	19.2	38.0	49.7	145
Fitting of the experimental OEC:					
$k_{YA} \times 10^2$ (s^{-1})	0.42	0.45	0.35	0.33	0.75
$k_{XA} \times 10^3$ (s^{-1})	0.010	0.003	0.007	0.010	0.134
AARD (%)*	6.62	11.4	8.02	10.3	6.62

678

679 $^{*}AARD = \frac{1}{N}\sum \left|\frac{experimental\ \ yield - calculated\ \ yield}{experimental\ \ yield}\right|$

680

Figure 1. Schematic diagram of Thar SFE pilot and semi industrial plants (1a = laboratory and pilot plant; 1b= semi-industrial plant). Nomenclature: A, B and C are extraction cells with volumes of = 2.7×10^{-4} m^3, B= 1.35×10^{-3} m^3 and 5.19×10^{-3} m^3, respectively; D= CO_2 storage tank; E= CO_2 Pump; F= Heat Exchanger; G= Automatic BPR Valve; H= Cyclonic Separator; I= BPR Valve; J= Pass valves; K= Condensers; L= Cooling System; M= Demister; N= Filter; P= Manometers; Q = Volume indicator; R= Flow meter; (⋯) Dotted line means PLC control; (---) Dashed lines means recycling.

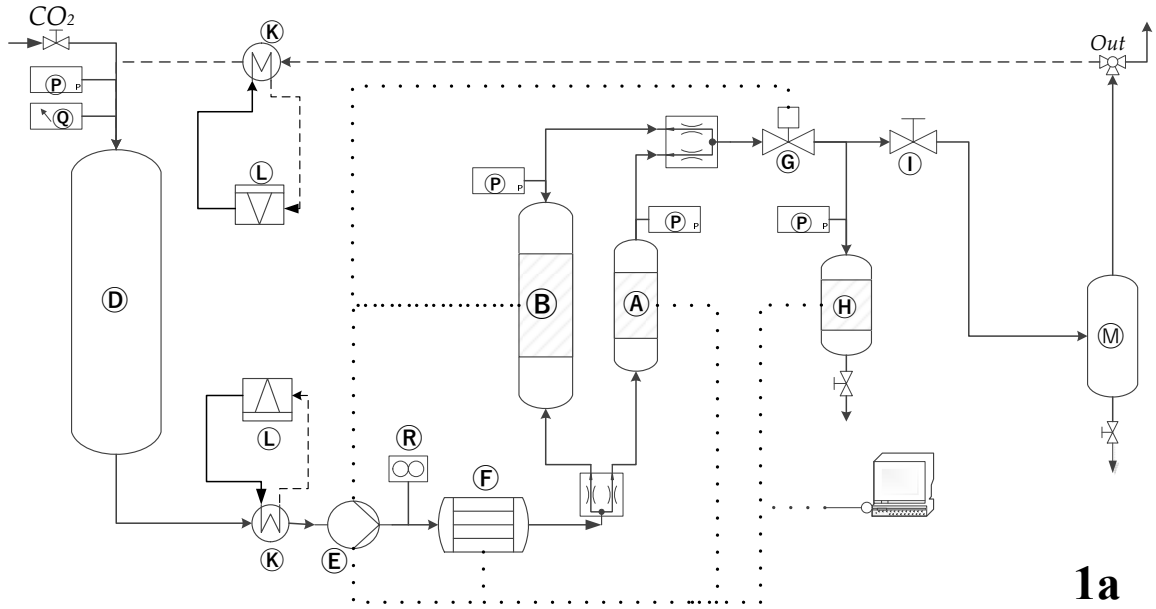

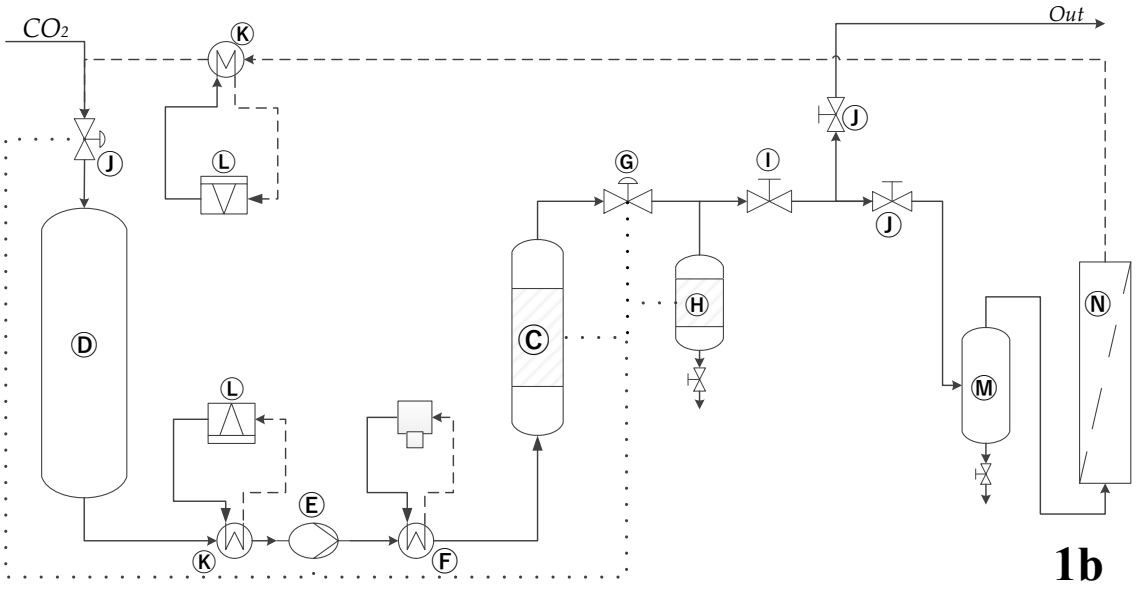

Figure 2. Overall extraction curves obtained using vessel V_A (2.7×10^{-4} m^3) and 0.090 kg of marigold flowers. Extraction temperature was 313 K and total extraction time was 270 min. (■) 14 MPa, 2.5×10^{-4} $kg\cdot s^{-1}$; (▲) 14 MPa, 5.0×10^{-4} $kg\cdot s^{-1}$; (●) 14 MPa, 7.5×10^{-4} $kg\cdot s^{-1}$; (□) 24 MPa, 5.0×10^{-4} $kg\cdot s^{-1}$; (△) 34 MPa, 5.0×10^{-4} $kg\cdot s^{-1}$. Dashed lines represent the BIC model fitting.

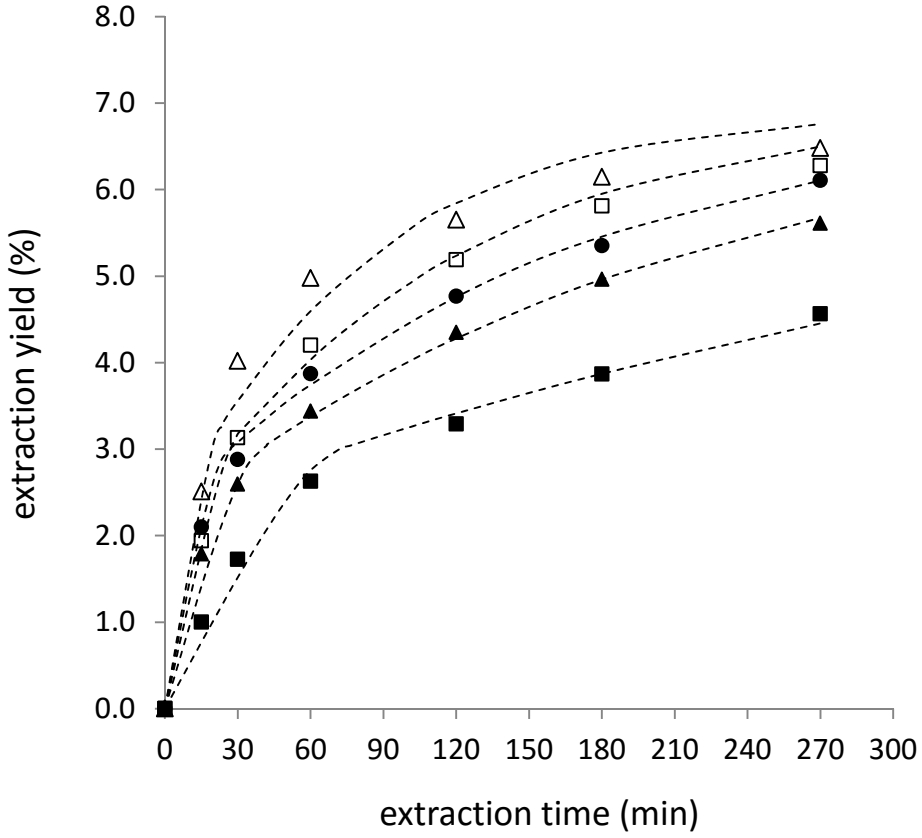

Figure 3. Total extractable material (X_o) and marigold solubility (Y^*) in supercritical CO_2 at 313 K and 14 MPa. Data represent the OECs obtained at 313 K and 14 MPa in V_A ($2.7x10^{-4}$ m^3) with different CO_2 flow rates Q = (■) 2.5×10^{-4} $kg\cdot s^{-1}$, (▲) 5.0×10^{-4} $kg\cdot s^{-1}$ and (●) 7.5×10^{-4} $kg\cdot s^{-1}$.

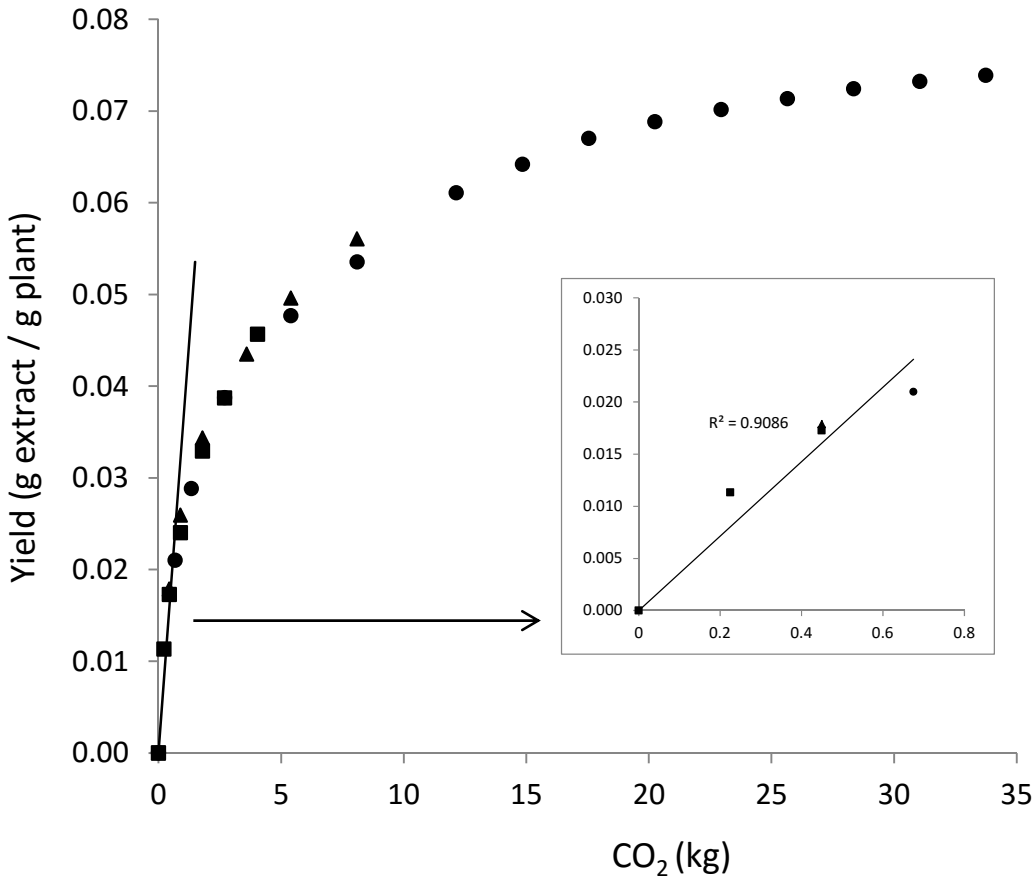

713 **Figure 4.** Marigold SFE scaling up at 313 K, 14 MPa and constant bed porosity (ε = 0.763)
714 from V_A to V_B (scaling factor = 4.95). Grey and black lines represent BIC predictions using
715 the criterions of keeping constant solvent velocity (Eq. (12)) and by keeping constant
716 residence time (Eq. (14)), respectively: (---) CER period; (––) FER period; (–·–) DC period.
717 Symbols represent experimental data: (■) laboratory scale V_A, $Q = 2.5\times10^{-4}$ kg·s^{-1}; (▲) pilot
718 scale, V_B, using Eq. (12); (△) pilot scale, V_B, using Eq. (14).
719

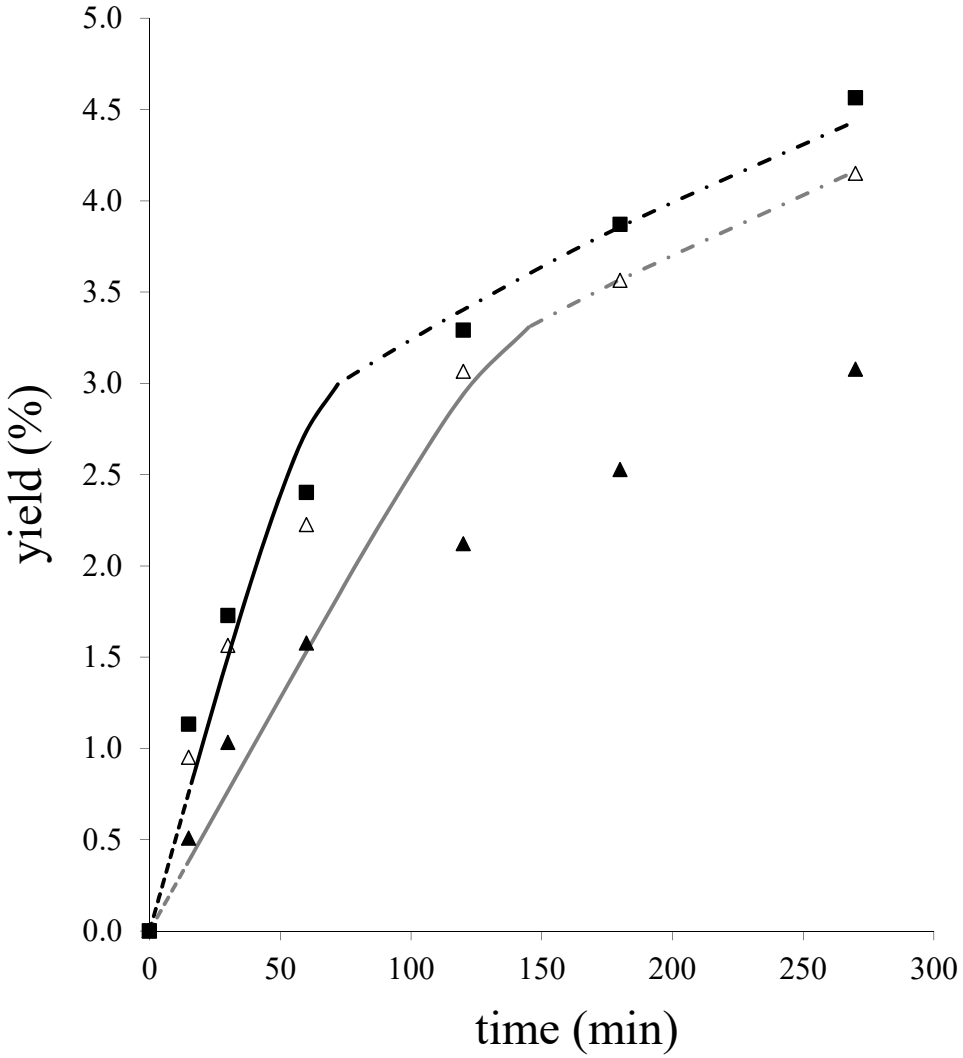

720
721

Figure 5. Marigold SFE scaling up at 313 K, 14 MPa and constant bed porosity (ε = 0.763) from V_A to V_C (scaling factor = 19.08). Grey and black lines represent BIC predictions using Eq. (12) and Eq. (14), respectively: (---) CER period; (––) FER period; (–·–) DC period. Symbols represent experimental data: (■) V_A, $Q = 2.5\times10^{-4}$ kg·s^{-1}; (○) V_C, Eq. (12); (●) V_C, Eq. (14).

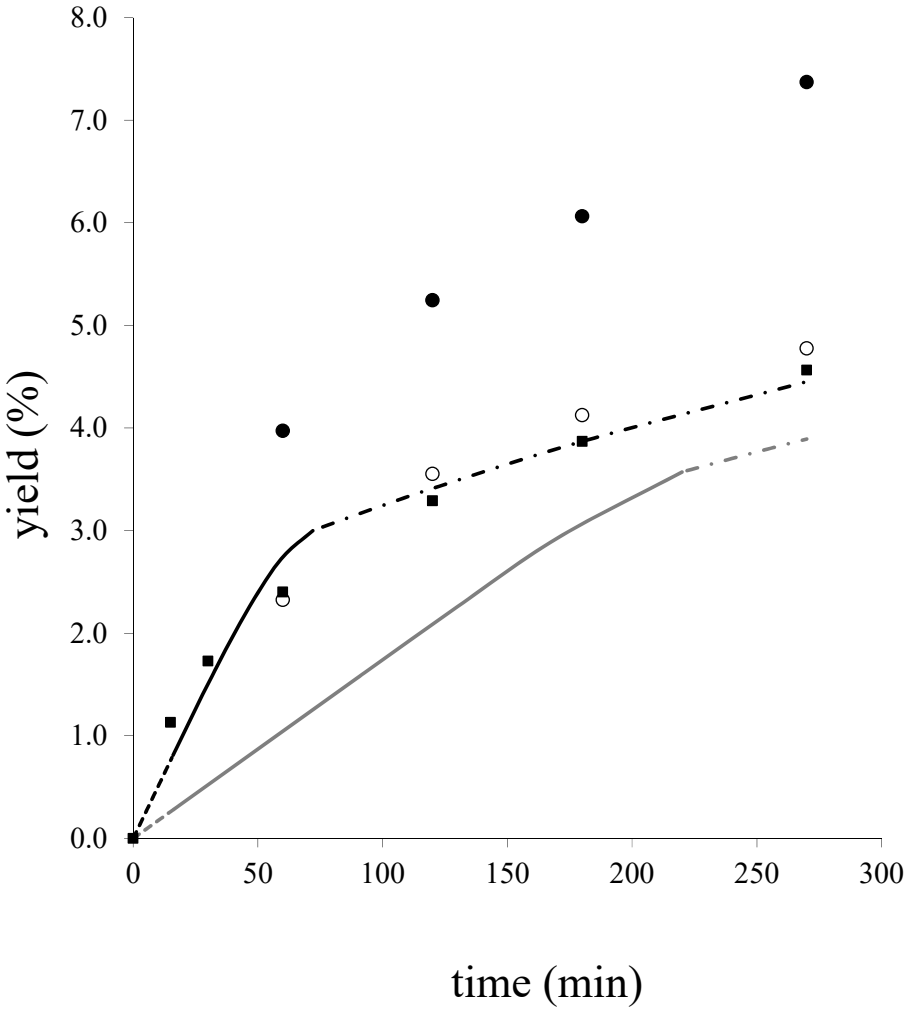

Figure 6. Correlating the fluid phase mass transfer coefficients k_{YA} of marigold experimental OECs with process parameters (Q and Sc number) and vessel geometrical constants (D and L). (△) V_A, 14 MPa; (▲) V_A, 24 and 34 MPa; (■) V_B, 14 MPa; (●) V_C, 14 MPa.